

## Comparative study of calix[4]arene derivatives: implications for ligand design

Jooyeon Hong, Sihyun Ham\*

*Department of Chemistry, Sookmyung Women's University, Seoul 140-742, Republic of Korea*

Received 31 January 2008; accepted 12 February 2008

Available online 14 February 2008

### Abstract

The first comparative theoretical study of three parent calix[4]arene analogues (calix[4]arene, thiacalix[4]arene, and homooxacalix[4]arene) has been performed using molecular dynamic simulations and density functional theory (MPWB1K/6-311G\*\*//B3LYP/6-311G\*\*) methods. The theoretical observations herein including optimized geometry, polarity, and atomic charge data provide that homooxacalix[4]arene would offer more efficient platform for metal ion recognition compared to thiacalix[4]arene or calix[4]arene.

© 2008 Elsevier Ltd. All rights reserved.

**Keywords:** Calix[4]arene; Thermodynamic stability; DFT calculation

Molecular recognition phenomena play a major role in the field of supramolecular chemistry and of biological processes. Molecular systems with preorganized and effectively functionalized recognition unit for guest molecules are ideal for host–guest interactions. In this regard, calixarenes **1**, composed of four phenol units connected by *ortho*-methylene bridges, provide particular promise due to their versatility and utility as complexation ability, conformational flexibility, and reactivity, and their applications in a wide diversity of areas as receptors, building blocks, ion transports, and sensors.<sup>1,2</sup> Recently, the replacement of the bridging methylene linkages by hetero atoms has attracted considerable interest on the new members of the calixarene family. Thiacalix[4]arenes **2** in the presence of sulfur atoms instead of methylene groups exhibit novel structural and functional features including easy oxidation of sulfur bridges and extra binding sites, which make these compounds very interesting with potential applications in host–guest chemistry.<sup>3–7</sup> Four distinctive conformations of thiacalix[4]arene are available as cone, partial cone, 1,2-alternate, and 1,3-alternate, as in the case of calix[4]-

arene. The different thiacalix[4]arene conformations have been achieved by appropriate functionalization. One of the most interesting features of the thiacalix[4]arene derivatives is metal ion shuttling through the aromatic cavity.<sup>8</sup> This phenomenon intrigued us to study the fundamental physical nature of the conformation features and the binding ability of the parent thiacalix[4]arene using more recent computational methods. On the other hand, tetrahomodioxacalix[4]arenes **3**, containing two extra oxygen atoms in the macrocyclic ring, can provide larger cavity, greater flexibility, and extra coordination sites for guest complexation compared to classical calix[4]arenes<sup>9–12</sup> (Fig. 1). Although tetrahomodioxacalix[4]arene derivatives have been synthesized and several experimental attempts have been made

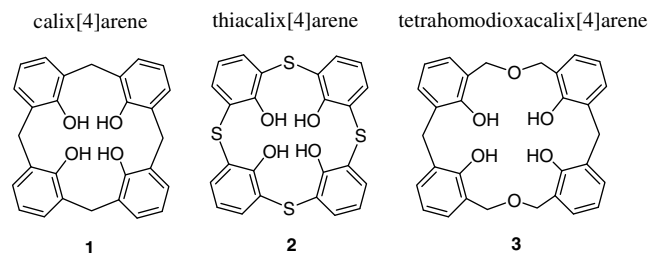


Fig. 1. Schematic representation of calix[4]arene derivatives.

\* Corresponding author. Tel.: +82 2 710 9410; fax: +82 2 710 9413.

E-mail address: [sihyun@sm.ac.kr](mailto:sihyun@sm.ac.kr) (S. Ham).

to determine the conformational preference depending on the substituents,<sup>13,14</sup> only one theoretical study on the conformational preference and thermodynamic stability for **3** was reported by us.<sup>15</sup> Here, we report the first comparative theoretical investigation on the conformational characteristics for three basic parent calix[4]arene analogues, **1–3**, by using molecular dynamics (MD) simulations and density functional theory (DFT) methods. The main purpose of this work is threefold. Firstly, it is to provide the subsequent comparison of thermodynamic stability sequence for three calix[4]arene derivatives with more recent and accurate DFT functional. Secondly, it is to give theoretical understanding of the physical nature and the stability order, which can be applied to understand the complexation behavior. Lastly, the theoretical results herein can be used to the experimental host design based on calix[4]arene macrocycles with various cavity sizes, depths, and polarity.

Despite the superior performance of DFT methods in numerous energy assessments and molecular structure predictions, there is increasing awareness that B3LYP can fail badly in describing the energies of non-bonded interactions, hydrogen bonded systems, and larger molecules.<sup>16</sup> Based on the recent work that the hybrid *meta*-GGA such as MPWB1K and MPW1B95 may provide more accurate assessments of weakly bound systems and better descriptions of intramolecular non-bonded interactions,<sup>17,18</sup> MPWB1K hybrid functional was chosen to compute the conformational equilibrium energy gap of calix[4]arene analogues and compared to the B3LYP functional.<sup>19</sup> While thiacalix[4]arene allows four conformations: cone, partial cone, 1,2-alternate, and 1,3-alternate similar to calix[4]arene (Figs. 2 and 3), tetrahomodioxacalix[4]arene can adopt five conformations with two different 1,2-alternate conformations, C-1,2-alternate and COC-1,2-alternate, as shown in Figure 4.<sup>13d</sup> The relative energies<sup>20</sup> for **1–3** are summarized in Tables 1–3.

The theoretically predicted stability order for **1** is cone > partial cone > 1,2-alternate > 1,3-alternate at the MPWB1K/6-311G\*\*//B3LYP/6-311G\*\* level (Table 1). It is different from the previous report that the stability order for 1,3-alternate and 1,2-alternate is reversed at the B3LYP/6-31G\* level.<sup>25a</sup> The lowest energy structure is optimized to be the cone (**1a**) and this is in agreement with the experimental observation.<sup>25b</sup> The cyclic array of intra-

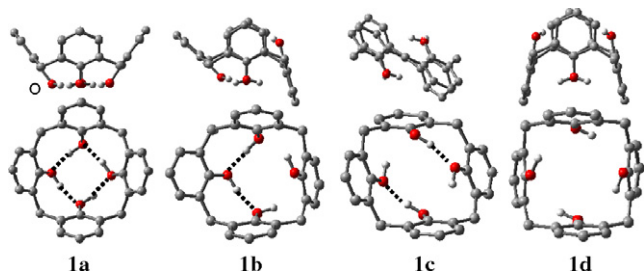


Fig. 2. Four available conformations of calix[4]arene optimized at the B3LYP/6-311G\*\* level are shown. For each structure, top and side views are displayed. Hydrogen bonds are shown in dashed lines at the top view. Hydrogen atoms are omitted for clarity except the phenolic hydrogens.

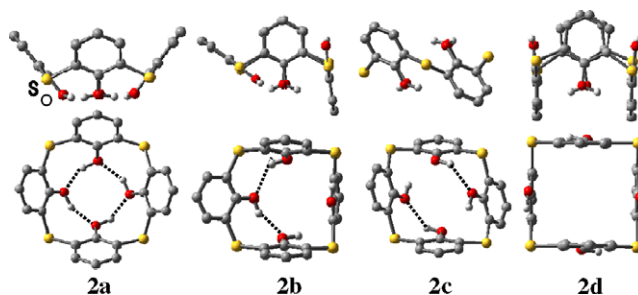


Fig. 3. Four available conformations of thiacalix[4]arene optimized at the B3LYP/6-311G\*\* level are shown. For each structure, top and side views are displayed. Hydrogen bonds are shown in dashed lines at the top view. Hydrogen atoms are omitted for clarity except the phenolic hydrogens.

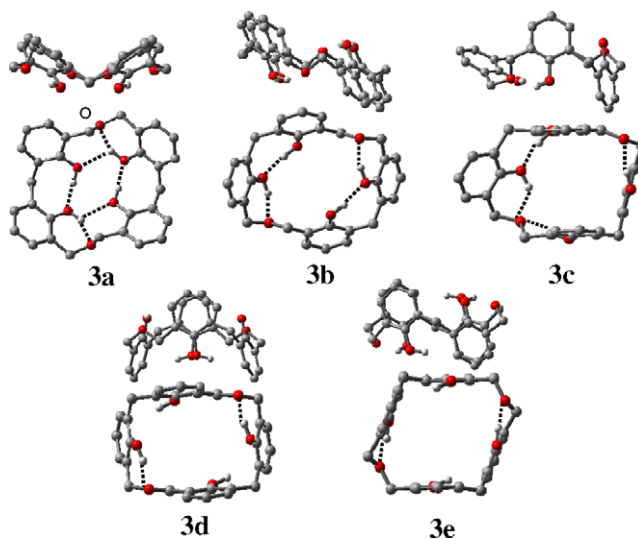


Fig. 4. Five available conformations of tetrahomodioxacalix[4]arene optimized at the B3LYP/6-311G\*\* level are shown. For each structure, top and side views are displayed. Hydrogen bonds are shown in dashed lines at the top view. Hydrogen atoms are omitted for clarity except the phenolic hydrogens.

Table 1  
Relative energies (kcal/mol) for **1** are listed at the B3LYP/6-311G\*\* and MPWB1K/6-311G\*\*//B3LYP/6-311G\*\* level of theory

	B3LYP/ 6-311G**	MPWB1K/ 6-311G** <sup>a</sup>	Dipole moment
Cone ( <b>1a</b> )	0.0	0.0	1.8
Partial cone ( <b>1b</b> )	9.2	7.3	1.0
1,2-Alternate ( <b>1c</b> )	12.2	10.6	0.0
1,3-Alternate ( <b>1d</b> )	15.5	12.1	0.0

Dipole moments (in D) calculated at the B3LYP/6-311G\*\* level are listed.

<sup>a</sup> Geometry optimized using B3LYP/6-311G\*\* level.

molecular hydrogen bonds in **1a** attributes to the thermal stability in a gas phase (Fig. 2). The average hydrogen bond distance between phenolic groups in **1a** is optimized to be 1.70 Å. The energy difference between **1a** and **1b** is 7.3 kcal/mol at the MPWB1K/6-311G\*\*//B3LYP/6-311G\*\* level, which is smaller to the energy gap determined by experiment.<sup>25b</sup> Direct comparison with experi-

Table 2

Relative energies (kcal/mol) for **2** are listed at the B3LYP/6-311G\*\* and MPWB1K/6-311G\*\*//B3LYP/6-311G\*\* level of theory

	B3LYP/ 6-311G**	MPWB1K/ 6-311G** <sup>a</sup>	Dipole moment
Cone ( <b>2a</b> )	0.0	0.0	5.7
Partial cone ( <b>2b</b> )	9.1	7.2	2.2
1,2-Alternate ( <b>2c</b> )	13.3	11.8	0.0
1,3-Alternate ( <b>2d</b> )	12.3	10.1	0.0

Dipole moments (in D) calculated at the B3LYP/6-311G\*\* level are listed.

<sup>a</sup> Geometry optimized using B3LYP/6-311G\*\* level.

Table 3

Relative energies (kcal/mol) for **3** are listed at the B3LYP/6-311G\*\* and MPWB1K/6-311G\*\*//B3LYP/6-311G\*\* level of theory

	B3LYP/ 6-311G**	MPWB1K/ 6-311G** <sup>a</sup>	Dipole moment
Cone ( <b>3a</b> )	0.0	0.0	2.2
Partial cone ( <b>3b</b> )	9.1	8.5	4.4
C-1,2-Alternate ( <b>3c</b> )	1.8	3.0	0.0
1,3-Alternate ( <b>3d</b> )	10.8	14.1	0.0
COC-1,2-Alternate ( <b>3a</b> )	18.5	19.2	0.0

Dipole moments (in D) calculated at the B3LYP/6-311G\*\* level are listed.

<sup>a</sup> Geometry optimized using B3LYP/6-311G\*\* level.

mental data is not valid due to the solvent effect in experimental data. All structural parameters of **1a** are in excellent agreement with the X-ray data<sup>25b</sup> that the average differences between X-ray and B3LYP/6-311G\*\* optimized geometry in bond distances and in angles are within 0.01 Å and 2°, respectively.

The first synthesis of **2** was reported in 1998 and X-ray diffraction study revealed that **2** adopts a cone conformation in the solid state.<sup>3</sup> The theoretically predicted stability order for **2** is cone > partial cone > 1,3-alternate > 1,2-alternate and this order is in agreement with the previous work<sup>7a</sup> although the MPWB1K/6-311G\*\* functional<sup>17</sup> reduces the energy gap between the conformers. The structural parameters of **2a** are in excellent agreement with the X-ray data<sup>3</sup> that the average differences between X-ray and B3LYP/6-311G\*\* optimized geometry in bond distances and in angles are within 0.02 Å and 1°, respectively. Despite the highest dipole (5.7 D), **2a** is 7.2 kcal/mol lower in energy than the second most stable conformer, **2b**. As shown in Figure 3, the cavity shape of **2a** is very similar to that of **1a** with fourfold symmetry. The average H bond distance between phenolic groups in **2a** is 1.87 Å, which is a bit longer than that in **1a** indicating larger cavity size of **2a**. The CHELPG atomic charge<sup>26</sup> computed for sulfur atoms (−0.15e) in **2a** implies that thiacalix[4]arene may offer extra binding sites for metal ion recognition. Overall, introducing sulfur atoms in a cavity induces higher dipole, larger cavity size, accordingly longer hydrogen bonding between phenolic groups, resulting in greater flexibility and polarity in thiacalix[4]arene compared to calix[4]arene.

Although the crystal structure for tetrahomodioxo *p*-*t*-butylcalix[4]arene was reported to adopt a distorted

cone,<sup>12a</sup> no experimental structure has been reported for the simplest form of tetrahomodioxacalix[4]arene, **3a**, due to its synthetic difficulty. The theoretically predicted order of stability for **3** is cone > C-1,2-alternate > partial cone > 1,3-alternate > COC-1,2-alternate and it is in agreement with the previous B3LYP/6-31G\*\*//RHF/6-31G\* calculation result.<sup>15</sup> As shown in Figure 4, the most stable conformer **3a** adopts the orientation that allows the formation of a cyclic array of intramolecular H bonds in the cavity. Four phenolic groups in a macrocycle of **3a** act simultaneously as donor and acceptor to form four hydrogen bonds with a distance of 1.79 or 2.33 Å. Additionally, two ether linkages in the cavity allow two hydrogen bonds with phenolic hydrogen with a distance of 1.98 Å. Overall, the shape of the cone is distorted by the formation of six hydrogen bonding array including two bifurcated hydrogen bonds.

The second lowest energy-minima structure for **3** is found to be C-1,2-alternate, **3c**. The distorted geometry due to −CH<sub>2</sub>OCH<sub>2</sub>− linkage is reserved to allow four hydrogen bonds (1.80 Å in average) between the phenolic hydrogen and the ether oxygen, but the cyclic H bonding array linking the four phenolic groups is no longer available in **3c**. The shape of **3c** is characterized to maximize the number of H bonds and to minimize the electrostatic repulsion between phenol rings. Overall, **3c** is 3.0 kcal/mol higher in energy than that for **3a**. The partial cone, **3b**, is found to be 8.5 kcal/mol higher in energy than that for **3a**. Although there are four H bonds (1.91 Å in average) in **3b**, unavoidable electrostatic repulsions to maximize H bonds contribute to the high energy and large dipole moment. The CHELPG charge<sup>26</sup> for ether oxygens in **3a** is computed to be quite negative (−0.44e). The theoretical observations herein including optimized geometry, polarity, and atomic charge data provide that tetrahomodioxacalix[4]arene would offer tighter binding and more effective cavity for metal ion recognition compared to thiacalix[4]arene or calix[4]arene.

In summary, the first comparative study on the conformational features and relative thermodynamic stabilities of calix[4]arene, thiacalix[4]arene, tetrahomodioxacalix[4]arene has been performed using molecular dynamics simulations and density functional theory (MPWB1K/6-311G\*\*//B3LYP/6-311G\*\*) in a gas phase. The recent hybrid *meta*-GGA functional, MPWB1K, was used for more accurate assessment for the relative stability of adoptable conformers. The cone is computed to be the most stable in all cases, in accordance with the available experimental observations. The substitution of methylene group with sulfur atom or dimethyleneoxa bridge induces the larger cavity size, conformational mobility, and polarity. Introducing the dimethyleneoxa bridges in the macrocycle (**3**) additionally increases the number of hydrogen bonding patterns and provides more efficient platform for metal ion recognition due to the extra oxygen binding sites. The conformational analyses show that the geometry and stability of the conformation are mainly determined by

the intramolecular hydrogen bonding patterns displayed by the phenolic groups and potential hydrogen acceptors in the cavity.

### Acknowledgment

This work was supported by the Sookmyung Women's University Research Grant, 2005.

### Supplementary data

Structural parameters for the cone conformations of **1–3** optimized at the B3LYP/6-311G\*\* level are available. Supplementary data associated with this article can be found, in the online version, at doi:10.1016/j.tetlet.2008.02.061.

### References and notes

- Asfari, Z.; Bohmer, V.; Harrowfield, J.; Vicens, J. *Calixarenes 2001*; Kluwer Academic: Dordrecht, 2001.
- Gutsche, C. D. *Calixarenes Revisited*; Royal Society of Chemistry: Cambridge, 1998.
- Akdas, H.; Bringel, L.; Graf, E.; Hosseini, M. W.; Mislin, G.; Pansanel, J.; De Cian, A.; Fischer, J. *Tetrahedron Lett.* **1998**, *39*, 2311–2314.
- Morohashi, N.; Iki, N.; Sugawara, A.; Miyano, S. *Tetrahedron* **2001**, *57*, 5557–5563.
- Lamartine, R.; Bavoux, C.; Vocanson, F.; Martin, A.; Senlis, G.; Perrin, M. *Tetrahedron Lett.* **2001**, *42*, 1021–1024.
- (a) Lhoták, P. *Eur. J. Org. Chem.* **2004**, 1675–1692; (b) Shokova, E. A.; Kovalev, V. V. *Russ. Chem. Bull.* **2003**, *39*, 13–40; (c) Morohashi, N.; Narumi, F.; Iki, N.; Hattori, T.; Miyano, S. *Chem. Rev.* **2006**, *106*, 5291–5316; (d) Iki, N.; Miyano, S. *J. Inclusion Phenom. Macro. Chem.* **2001**, *41*, 99–105.
- (a) Bernardino, R. J.; Costa Cabral, B. J. *J. Mol. Struct.-Theochem* **2001**, *549*, 253–260; (b) Suwattanamala, A.; Magalhães, A. L.; Gomes, J. A. N. F. *Chem. Phys. Lett.* **2004**, *385*, 368–373.
- Lee, J. K.; Kim, S. K.; Bartsch, R. A.; Vicens, J.; Miyano, S.; Kim, J. S. *J. Org. Chem.* **2003**, *68*, 6720–6725.
- (a) Gutsche, C. D.; Dhawan, B.; No, K. H.; Muthukrishnan, R. *J. Am. Chem. Soc.* **1981**, *103*, 3782–3792; (b) Dhawan, B.; Gutsche, C. D. *J. Org. Chem.* **1983**, *48*, 1536–1539; (c) Gutsche, C. D.; Bauer, L. J. *J. Am. Chem. Soc.* **1985**, *107*, 6059–6063.
- (a) Masci, B.; Saccheo, S. *Tetrahedron* **1993**, *49*, 10739–10748; (b) De Iasi, G.; Masci, B. *Tetrahedron Lett.* **1993**, *34*, 6635–6638; (c) Masci, B. *Tetrahedron* **1995**, *51*, 5459–5464.
- Masci, B.; Finelli, M.; Varrone, M. *Chem. Eur. J.* **1998**, *4*, 2018–2030.
- (a) Thuéry, P.; Nierlich, M.; Vicens, J.; Masci, B.; Takemura, H. *Eur. J. Inorg. Chem.* **2001**, 637–643; (b) Thuéry, P.; Nierlich, M.; Vicens, J.; Masci, B. *Acta Crystallogr., Sect. C* **2001**, *57*, 70–71.
- (a) No, K. H. *Bull. Korean Chem. Soc.* **1999**, *20*, 33–34; (b) No, K. H.; Park, Y. J.; Choi, E. J. *Bull. Korean Chem. Soc.* **1999**, *20*, 905–909; (c) No, K.; Kim, J. S.; Shon, O. J.; Yang, S. H.; Suh, I. H.; Kim, J. G.; Bartsch, R. A.; Kim, J. Y. *J. Org. Chem.* **2001**, *66*, 5976–5980; (d) No, K.; Lee, J. H.; Yang, S. H.; Yu, S. H.; Cho, M. H.; Kim, M. J.; Kim, J. S. *J. Org. Chem.* **2002**, *67*, 3165–3168; (e) No, K.; Chung, H. J.; Yu, H. J.; Yang, S. H.; Noh, K. H.; Thuéry, P.; Vicens, J.; Kim, J. S. *J. Inclusion Phenom. Macro. Chem.* **2003**, *46*, 97–103; (f) No, K.; Bok, J. H.; Suh, I. H.; Kang, S. O.; Ko, J.; Nam, K. C.; Kim, J. S. *J. Org. Chem.* **2004**, *69*, 6938–6941; (g) Choi, J. K.; Lee, A.; Kim, S.; Ham, S.; No, K.; Kim, J. S. *Org. Lett.* **2006**, *8*, 1601–1604.
- (a) Masci, B. *J. Org. Chem.* **2001**, *66*, 1497–1499; (b) Masci, B.; Gabrielli, M.; Mortera, S. L.; Nierlich, M.; Thuéry, P. *Polyhedron* **2002**, *21*, 1125–1131.
- Ham, S. *Bull. Korean Chem. Soc.* **2004**, *25*, 1911–1916.
- (a) Lynch, B. J.; Fast, P. L.; Harris, M.; Truhlar, D. G. *J. Phys. Chem. A* **2000**, *104*, 4811–4815; (b) Zhao, Y.; Tishchenko, O.; Truhlar, D. G. *J. Phys. Chem. B* **2005**, *109*, 19046–19051; (c) Tsuzuki, S.; Lüthi, H. P. *J. Chem. Phys.* **2001**, *114*, 3949–3957; (d) Schreiner, P. R.; Fokin, A. A.; Pascal, R. A.; Meijere, A. *Org. Lett.* **2006**, *8*, 3635–3638.
- Zhao, Y.; Truhlar, D. G. *J. Phys. Chem. A* **2004**, *108*, 6908–6918.
- Wodrich, M. D.; Corminboeuf, C.; von Schleyer, P. R. *Org. Lett.* **2006**, *8*, 3631–3634.
- Becke, A. D. *J. Chem. Phys.* **1993**, *98*, 5648–5652.
- All energy calculations and geometry optimizations were performed using the GAUSSIAN 03 package.<sup>21</sup> To search the global minima structures for each conformer, the following procedure was executed. An initial conformational analysis for each molecular system was first performed by molecular dynamics (MD) simulations with AMBER 9 program package using the ff99 force field.<sup>22</sup> The molecular system was subject to 1000 steps of conjugate gradient energy minimization, and then brought into an equilibrium state for 100 ps using the Berendsen coupling algorithm.<sup>23</sup> In all calculations, an 8.0 Å non-bonded interaction cut-off was used and non-bonded pair lists were updated every 20 integration steps. A 2 fs time step was used for the simulation. The simulation was performed for 1000 ps at 800 K and the structures were saved every 5 ps for analyses. From the MD simulation trajectory, total 200 structures were collected, which were then subjected to the following optimization procedure using AM1 semi-empirical method<sup>24</sup> to find the energy minima that would be used as initial structures for the density functional theory (DFT) calculations. The DFT calculations were performed B3LYP functional<sup>19</sup> with 3-21G\*, 6-31G\*\*, and 6-311G\*\* basis sets followed by vibrational analysis to verify the identity of each stationary point as a minimum. Single point energy calculation was executed at the MPWB1K/6-311G\*\* level using B3LYP/6-311G\*\* optimized geometry.
- Frisch, M. J.; Trucks, G. W.; Schlegel, H. B.; Scuseria, G. E.; Robb, M. A.; Cheeseman, J. R.; Montgomery, J. A., Jr.; Vreven, T.; Kudin, K.; Burant, J. C.; Millam, J. M.; Iyengar, S. S.; Tomasi, J.; Barone, V.; Mennucci, B.; Cossi, M.; Scalmani, G.; Rega, N.; Petersson, G. A.; Nakatsuji, H.; Hada, M.; Ehara, M.; Toyota, K.; Fukuda, R.; Hasegawa, J.; Ishida, M.; Nakajima, T.; Honda, Y.; Kitao, O.; Nakai, H.; Klene, M.; Li, X.; Knox, J. E.; Hratchian, H. P.; Cross, J. B.; Adamo, C.; Jaramillo, J.; Comperts, R.; Startmann, R. E.; Yazyev, O.; Austin, A. J.; Cammi, R.; Pomelli, C.; Ochterski, J. W.; Ayala, P. Y.; Morokuma, K.; Voth, G. A.; Salvador, P.; Dannenberg, J. J.; Zakrzewski, V. G.; Dapprich, S.; Daniels, A. D.; Strain, M. C.; Farkas, O.; Malick, D. K.; Rabuck, A. D.; Raghavachari, K.; Foresman, J. B.; Ortiz, J. V.; Cui, Q.; Baboul, A. G.; Clifford, S.; Cioslowski, J.; Stefanov, B. B.; Liu, G.; Liashenko, A.; Piskorz, P.; Komaromi, I.; Martin, R. L.; Fox, D. J.; Keith, T.; Al-Laham, M. A.; Peng, C. Y.; Nanayakkara, A.; Challacombe, M.; Gill, P. M. W.; Johnson, B.; Chen, W.; Wong, M. W.; Gonzalez, C.; Pople, J. A. GAUSSIAN 03, revision C.02 Gaussian, Inc.: Wallingford CT, 2004.
- Case, D. A.; Pearlman, D. A.; Caldwell, J. W. et al. AMBER 9; University of California, San Francisco, 2002.
- Berendsen, H. J. C.; Postma, J. P. M.; van Gunsteren, W. F.; DiNola, A.; Haak, J. R. *J. Chem. Phys.* **1984**, *81*, 3684–3690.
- (a) Sudmeier, J. L.; Bell, S. J. *J. Am. Chem. Soc.* **1977**, *99*, 4499–4500; (b) Dewar, M.; Zoebisch, E. G.; Healy, E. F. *J. Am. Chem. Soc.* **1985**, *107*, 3902–3909.
- (a) Bernardino, R. J.; Costa Cabral, B. J. *J. Phys. Chem. A* **1999**, *103*, 9080–9085; (b) Ungaro, R.; Pochini, A.; Andreetti, G. D.; Snagernano, V. *J. Chem. Soc., Perkin Trans. 2* **1984**, 1979–1985.
- Breneman, C. M.; Wiberg, K. B. *J. Comput. Chem.* **1990**, *11*, 361–373.